Advanced Functional Materials

Bioengineered Porous Silicon Nanoparticles@Macrophages Cell Membrane as Composite Platforms for Rheumatoid Arthritis

--Manuscript Draft--

Manuscript Number:	adfm.201801355R1
Full Title:	Bioengineered Porous Silicon Nanoparticles@Macrophages Cell Membrane as Composite Platforms for Rheumatoid Arthritis
Article Type:	Full Paper
Section/Category:	
Keywords:	cell membrane; porous silicon; Nanoparticles; macrophages; autoimmune diseases
Corresponding Author:	Helder Santos, D.Sc. (Chem. Eng.) University of Helsinki Helsinki, Helsinki FINLAND
Additional Information:	
Question	**Response**
Please submit a plain text version of your cover letter here. **If you are submitting a revision of your manuscript, please do not overwrite your original cover letter. There is an opportunity for you to provide your responses to the reviewers later; please do not add them here**.	Dr. Jos Lenders Editor Advanced Functional Materials Dear Dr. Lenders, I would like to submit our manuscript entitled “Bioengineered Porous Silicon Nanoparticles@Macrophages Cell Membrane as Composite Platforms for Rheumatoid Arthritis” by our group and collaborators for publication as a full paper in Advanced Functional Materials. Biohybrid vectors are becoming increasingly popular in the nanotechnology field. The applications of such nanoparticles (NPs) range from vaccines for cancer therapy, to toxin detoxification systems, to drug delivery systems, and to artificial organelles. Autoimmune diseases develop when the body loses the tolerance towards the “self”, initiating an immune response against cells or tissues. Rheumatoid arthritis (RA) represents an autoimmune disease attacking the joints, leading to loss of function and co-morbidities. The current treatments are based on the administration of immunosuppressive agents or disease modifying drugs, all presenting systemic side effects. Exploiting the advantages brought by the nanosize, NPs have been proposed for the local delivery of therapeutics, through the extravasation through leaky vasculature and sequestration by immune cells effect or being directly targeted to folate receptor, to the site of diseases and to the cells involved in the diseases (e.g., macrophages). Moreover, NPs have been employed in the induction of immune tolerance against self-reactive peptides in several autoimmune diseases, including RA. Thereby, keeping in mind a future application of the developed platform for drug delivery or vaccination for autoimmune diseases (and rheumatoid arthritis in particular), KG-1 macrophages were selected as model cell source for the cytoplasmic membrane vesicles. Macrophages are identified as one of the key players in the inflammation of the joints, showing a complex population heterogeneity and serving as possible target of future therapies aimed to their polarization towards an anti-inflammatory phenotype. Here, we developed composite platforms made of PSi coated with cell membrane vesicles derived from macrophages, investigating the parameters leading to stable systems. Moreover, we analyzed these systems in terms of size, surface morphology, and stability in different biological buffers, followed by the biological evaluation of cytocompatibility and immunological profile. A study of the parameters influencing the production of PSi@cytoplasmic membranes was conducted. Positively charged PSi NPs showed a lower degree of encapsulation

	due to the strong electrostatic interactions between the particles and the cell membranes. As for the differences in the hydrophobicity of the surface of the NPs, they had an impact on the choice of the medium employed in the extrusion and in the additional procedures (tip sonication) required. The nanoplatforms showed acceptable stability in physiological buffers, while in plasma and simulated synovial fluid greatly enhanced the stability of the hydrophobic particles (UnTHCPSi). Moreover, the cytocompatibility of the systems evaluated in different cell lines representing the cells present in the target organs, blood vessel and the kidney and liver. The nanoplatforms were compatible up to 48 h at concentrations ranging from 0.5 to 50 µg/mL. Finally, the immunological profile investigated in KG-1 macrophages showed that PSi@KG-1 nanosystem did not result in the activation of the immune system and the coating of UnTHCPSi particles with cell membranes attenuated the immunostimulative potential of the particles. Overall, we developed, as proof of concept, two biohybrid cytocompatible nanoplatforms as potential drug delivery systems or as antigen carriers for the induction of tolerance against autoimmune diseases. This work brings together several scientific areas, including materials science, biomedical engineering, biomaterials, and rheumatoid arthritis. This new result is completely covered within the scope of Advanced Functional Materials and is of timely interest to the readers of this journal. We firmly believe that this manuscript is suitable for publishing in Advanced Functional Materials. We truly declare that the present article and its contents have not been previously published in any language anywhere by any of the present authors and are not also under simultaneous consideration in another journal at the time of this submission. Thank you for your consideration. Sincerely yours, Hélder Santos Dr. Hélder A. Santos, D.Sc. (Chem. Eng.), Associate Professor, Group Leader, Head Division Head of the Division of Pharmaceutical Chemistry and Technology, Faculty of Pharmacy Head of Preclinical Drug Formulation and Analysis Group Head of the Nanomedicines and Biomedical Engineering Group Drug Research Program, Faculty of Pharmacy, University of Helsinki, Finland; & Helsinki Institute of Life Science (HiLIFE), University of Helsinki, Finland @ Email: helder.santos@helsinki.fi, http://www.helsinki.fi/~hsantos/ https://scholar.google.com/citations?hl=en-EN&user=K3Pj_gwAAAAJ
Do you or any of your co-authors have a conflict of interest to declare?	No. The authors declare no conflict of interest.
Corresponding Author Secondary Information:	
Corresponding Author's Institution:	University of Helsinki
Corresponding Author's Secondary Institution:	
First Author:	Flavia Fontana
First Author Secondary Information:	
Order of Authors:	Flavia Fontana
	Silvia Albertini
	Alexandra Correia

	Marianna Kemell
	Rici Lindgren
	Ermei Mäkilä
	Jarno Salonen
	Jouni Hirvonen
	Franca Ferrari
	Helder Santos, D.Sc. (Chem. Eng.)
Order of Authors Secondary Information:	
Abstract:	Biohybrid nanosystems are at the center of personalized medicine, affording prolonged circulation time and targeting to the disease site, and serving as antigenic sources of vaccines. The optimization and functionality parameters of these nanosystems vary depending on the properties of the core particles. In this work, the effects of the core particles' surface charge and hydrophobicity are evaluated on the nanosystem coating with vesicles derived from plasma membrane. The measured parameters are the dimensions, surface charge, shape, and stability of the biohybrid nanosystems, both in buffer and in biologically relevant media (plasma and simulated synovial fluid). Moreover, the cytocompatibility properties of the developed nanosystems are evaluated in different cell lines mimicking the target cell populations and other districts of the body involved in the distribution and elimination of the nanoparticles. Finally, the immunological profile of the particles is investigated, highlighting the absence of immune activation promoted by the nanoplatforms.

WILEY-VCH

DOI: 10.1002/ ((please add manuscript number))
Article type: Full Paper

Bioengineered Porous Silicon Nanoparticles@Macrophages Cell Membrane as Composite Platforms for Rheumatoid Arthritis

Flavia Fontana, Silvia Albertini, Alexandra Correia, Marianna Kemell, Rici Lindgren, Ermei Mäkilä, Jarno Salonen, Jouni T. Hirvonen, Franca Ferrari and Hélder A. Santos**

F. Fontana, S. Albertini, A. Correia, Prof. J. T. Hirvonen, Prof. H. A. Santos
Drug Research Program, Division of Pharmaceutical Chemistry and Technology, Faculty of Pharmacy, University of Helsinki, Helsinki FI-00014, Finland
email: flavia.fontana@helsinki.fi; helder.santos@helsinki.fi

S. Albertini, Prof. F. Ferrari
Department of Drug Sciences, University of Pavia, Pavia IT-27100, Italy

Dr. M. Kemell
Department of Chemistry, University of Helsinki, Helsinki FI-00014, Finland

R. Lindgren, E. Mäkilä, Prof. J. Salonen
Laboratory of Industrial Physics, Department of Physics and Astronomy, University of Turku, Turku FI-20014, Finland

Prof. H. A. Santos
Helsinki Institute of Life Science (HiLIFE), University of Helsinki, Helsinki FI-00014, Finland

Keywords: cell membrane; porous silicon; nanoparticles; macrophages; autoimmune diseases

Abstract

Biohybrid nanosystems are at the center of personalized medicine, affording prolonged circulation time and targeting to the disease site, and serving as antigenic sources of vaccines. The optimization and functionality parameters of these nanosystems vary depending on the properties of the core particles. In this work, the effects of the core particles' surface charge and hydrophobicity are evaluated on the nanosystem coating with vesicles derived from plasma membrane. The measured parameters are the dimensions, surface charge, shape, and stability of the biohybrid nanosystems, both in buffer and in biologically relevant media (plasma and simulated synovial fluid). Moreover, the cytocompatibility properties of the developed nanosystems are evaluated in different cell lines mimicking the target cell populations and other districts of the body involved in the distribution and elimination of the nanoparticles. Finally, the immunological profile of the particles is investigated, highlighting the absence of immune activation promoted by the nanoplatforms.

1. Introduction

Biohybrid vectors are becoming increasingly popular in the nanotechnology field. The applications of such nanoparticles (NPs) range from vaccines for cancer therapy, to toxin detoxification systems, to drug delivery systems, and to artificial organelles.[1] The biohybrid nanosystems can be obtained either by binding nanoparticles to cells (*e.g.*, red blood cells and T lymphocytes) or by coating the particles with vesicles derived from the cytoplasmic membrane.[2] Poly(D,L-lactide-co-glycolide) NPs and gold NPs/nanocages, all presenting as a common feature a negative surface potential, have been successfully encapsulated in red blood cells, platelets, and cancer cell membranes, displaying increased stability in plasma, extending the circulation time of the particles *in vivo*, targeting the tumor, or delivering tumor antigens to antigen presenting cells.[2a, 3]

Porous silicon (PSi) is an inorganic material displaying interesting properties in different biomedical applications from the enhancement of the dissolution rate of poorly soluble drugs, to the oral delivery of macromolecules for the therapy of diabetes, to treatment of cardiovascular diseases, to targeted cancer chemotherapy, to *in vivo* biohybrid drug delivery systems (leukolike vectors), to immunotherapy.[4] We previously reported two systems encapsulated in cell membrane vesicles: these systems differ in the nature of the core particles.[5] In one case, carboxylic acid terminated PSi particles were directly co-extruded together with the cell membranes, while in the other thermally oxidized PSi NPs were first encapsulated within a polymeric layer and, then, extruded with the cell membranes. We were intrigued by the need for extrusion in two different buffers (PBS pH 7.4 or purified water) for the two different systems, thereby we decided to systematically study the effect of surface charge and hydrophobicity on the preparation parameters of PSi@cell membrane particles (**Scheme 1**).

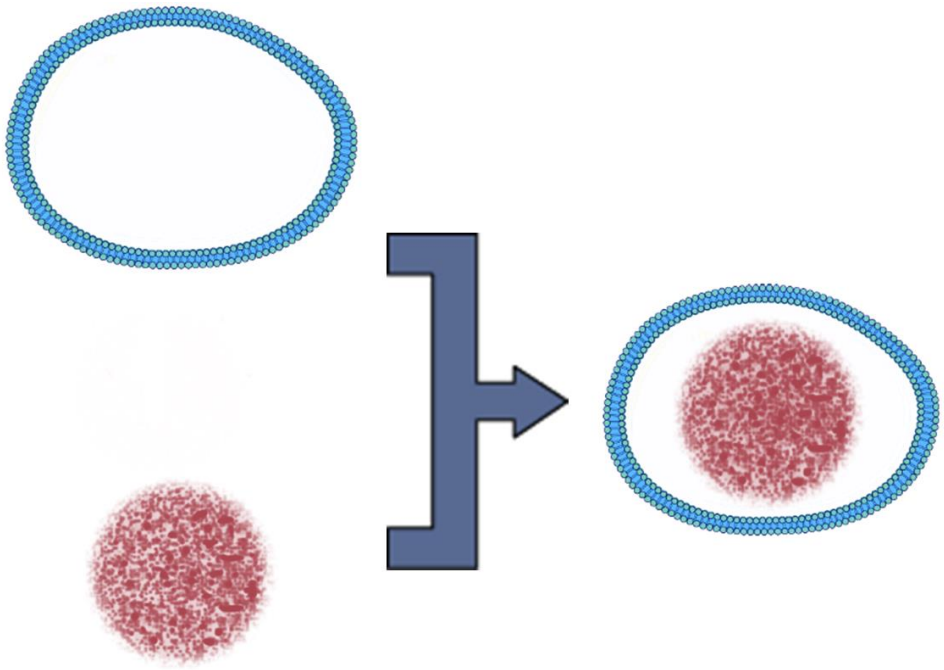

Scheme 1. Schematic of the nanoplatforms. PSi nanoparticles are processed together with cytoplasmic membranes isolated from KG-1 macrophages. Image created with Servier Medical Art.

Autoimmune diseases develop when the body loses the tolerance towards the "self", initiating an immune response against cells or tissues.[6] Rheumatoid arthritis (RA) represents an autoimmune disease attacking the joints, leading to loss of function and co-morbidities.[7] The current treatments are based on the administration of immunosuppressive agents or disease modifying drugs, all presenting systemic side effects.[6a, 7] Exploiting the advantages brought by the nanosize, NPs have been proposed for the local delivery of therapeutics, through the extravasation through leaky vasculature and sequestration by immune cells (ELVIS) effect or being directly targeted to folate receptor, to the site of diseases and to the cells involved in the diseases (*e.g.*, macrophages).[6b, 8] Moreover, NPs have been employed in the induction of immune tolerance against self-reactive peptides in several autoimmune diseases, including RA.[6b, 9]

Thereby, keeping in mind a future application of the developed platform for drug delivery or vaccination for autoimmune diseases (and rheumatoid arthritis in particular), KG-1 macrophages were selected as model cell source for the cytoplasmic membrane vesicles. Macrophages are identified as one of the key players in the inflammation of the joints, showing a complex population heterogeneity and serving as possible target of future therapies aimed to their polarization towards an anti-inflammatory phenotype.[10] Here, we developed composite platforms made of PSi coated with cell membrane vesicles derived from macrophages, investigating the parameters leading to stable systems. Moreover, we analyzed these systems in terms of size, surface morphology, and stability in different biological buffers, followed by the biological evaluation of cytocompatibility and immunological profile.

2. Results and Discussion

2.1. Development of the Platforms

Undecylenic acid modified thermally hydrocarbonized PSi (UnTHCPSi) NPs were selected as example of negatively charged hydrophobic particles, while (3-aminopropyl)-triethoxysilane modified thermally carbonized PSi (APTS-TCPSi) NPs served as positively charged nanosystem. Moreover, TCPSi NPs represented a negatively charged hydrophilic system.[4e] The properties of the NPs in terms of average size and number of particles in 1 mg are presented in **Table 2**. The process of development of the nanoplatforms included different extrusion buffers (sucrose 0.3 M and Milli-Q water), and the use of tip sonication in different stages of the preparation process. As shown in **Table 1**, in the case of the hydrophobic, negatively charged UnTHCPSi, the use of a stabilizer (sucrose) and of a double tipsonication were needed to obtain homogenous populations of NPs with an average hydrodynamic diameter of 302±188 nm, a PdI of 0.15±0.01, and a zeta (ζ)-potential of –23.7±0.2 mV. In the case of the positively charged NPs, APTS-TCPSi, the discriminating variable in the choice of the best parameters was the final surface charge of the system. We selected the nanosystem

that presented the inversion of charge to –6.3±1.1 mV (from the positive of APTS-TCPSi to a slightly negative one). These NPs had an average hydrodynamic diameter of 304±100 nm, with a PdI of 0.31±0.04. The optimal parameters for these NPs resulted the same as for UnTHCPSi particles (sucrose 0.3 M and two rounds of tip sonication).

As for the hydrophilic TCPSi NPs, Milli-Q water and a preliminary sonication to homogenously disperse the NPs before the extrusion were sufficient to obtain nanoplatforms with a size of 246±80 nm, a PdI of 0.18±0.03, and a negative surface charge with a ζ-potential of –22.1±5.2 mV.

Table 1. Nanoplatform development and the effect of the extrusion buffers and tipsonication in different stages of the preparation process (before extrusion, after extrusion, before and after extrusion) on NPs size, PdI, and ζ-potential. The nanoplatform chosen for the following experiments is identified by ++, while the outcome of the other variables is coded from – – (worst nanoplatform) to + (second best nanoplatform). The results of average size, PdI, and ζ-potential are presented as mean±s.d (*n=3*).

PSi NPs	Buffers	Tip Sonication	Size [nm]	PDI	ζ-potential [mV]	
APTS-TCPSi	Sucrose 0.3 M	Before	aggregated	/	+8.8±1.3	– –
		Before and After	304±100	0.30±0.040	–6.3±1.1	++
	Milli-Q water	Before	334±20	0.30±0.049	+31.2±0.5	+
		Before and After	aggregated	/	–5.7±7.1	–
UnTHCPSi	Sucrose 0.3 M	Before	575±200	0.50±0.07	–21.2±0.3	–
		Before and After	303±200	0.15±0.007	–23.7±0.2	++
	Milli-Q water	Before	649±300	0.24±0.2	–15.1±7.1	+
		Before and after	aggregated	/	–8.7±0.9	– –

TCPSi	Milli-Q water	No Sonication	410±180	0.5±0.1	–20.6±6.5	–
		After	aggregated	/	–19.8±4.9	– –
		Before	246±100	0.180±0.03	–22.1±5.2	++
	Sucrose 0.3 M	Before	289±100	0.3±0.07	–23.0±5.9	+

The shape of the nanoplatforms was then evaluated by transmission electron microscopy (TEM), as shown in **Figure 1**. The cell membrane encapsulation of APTS-TCPSi NPs was not complete (Figure 1a) as indicated also by the ζ-potential values. These NPs tend to aggregate (with dimensions > 1 µm) and the only partial cell membrane coating is clear from the difference in the surface shape between coated and uncoated regions. On the contrary, both for UnTHCPSi and TCPSi, the NPs were successfully encapsulated within the cytoplasmic membrane vesicles (Figure 1b and c). The size observed in TEM, analyzed with ImageJ, is in good agreement with the values obtained by dynamic light scattering (average of 450 nm for UnTHCPSi and 350 nm for TCPSi).

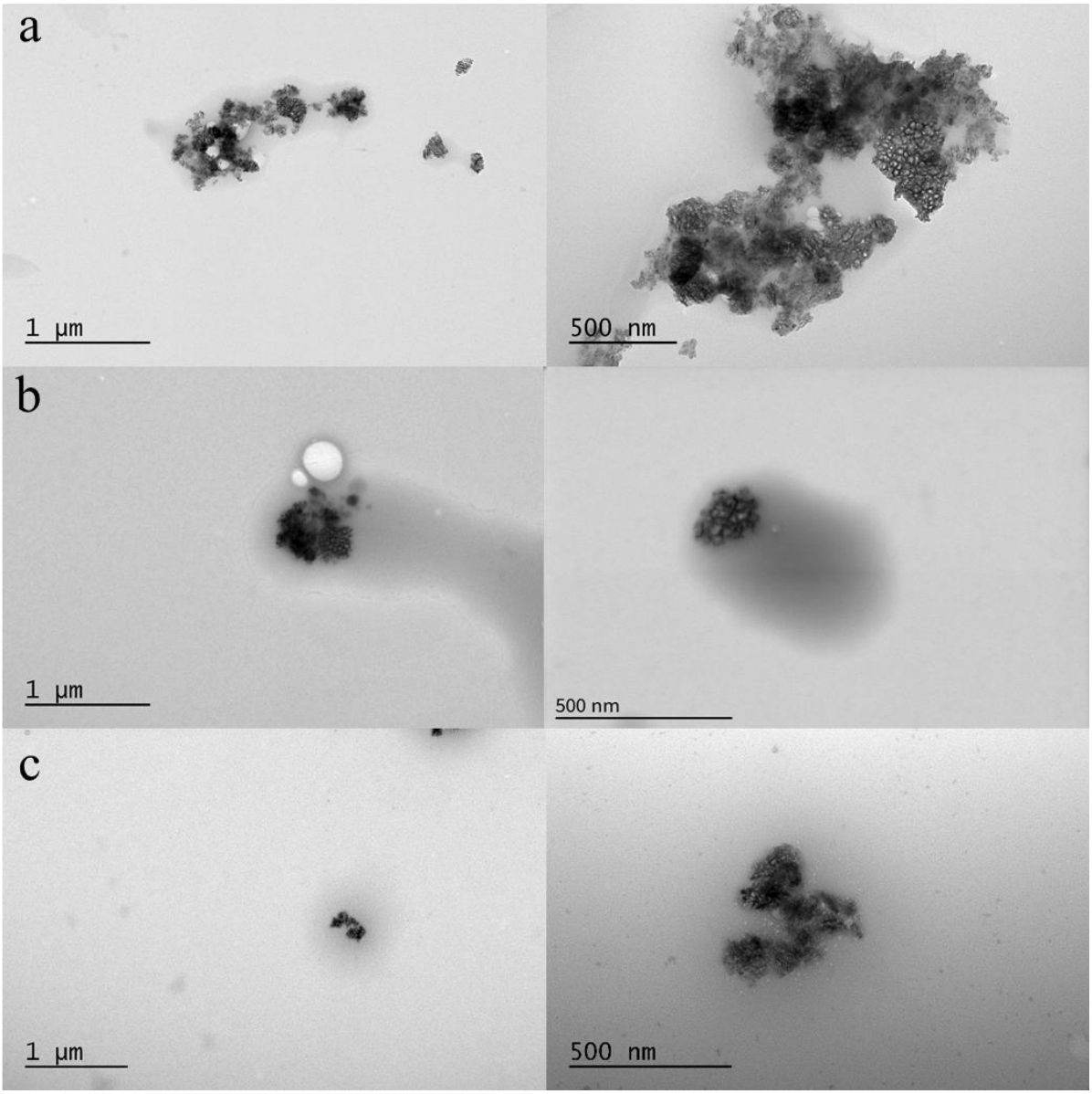

Figure 1. TEM micrographs of (a) APTS-TCPSi@KG-1, (b) UnTHCPSi@KG-1, and (c) TCPSi@KG-1.

Furthermore, with the aim of confirming the presence of the cell membrane on the surface of the particles, we analyzed the samples with energy dispersive X-ray analysis in scanning electron microscope (SEM–EDX) to highlight the elemental composition of the sample. As shown in **Figures S1-S3**, the presence of phosphorous (P), derived from the phospholipids of the membrane, could not be confirmed in any of the samples, despite the presence of the membrane in the pictures. The peak of silicon (Si), however, was clearly identified. We hypothesize that the thickness of the cell membrane layer is too thin, thereby the

concentration of P falls below the limit of detection of the instrument.[11] Thereby, in order to confirm the presence of the lipidic membrane, we quantified the amount of choline present in the samples (**Figure 2**). TCPSi@KG-1 NPs retain higher amount of phosphatidyl choline (2-fold higher, *p<0.0001*) compared to UnTHCPSi@KG-1.

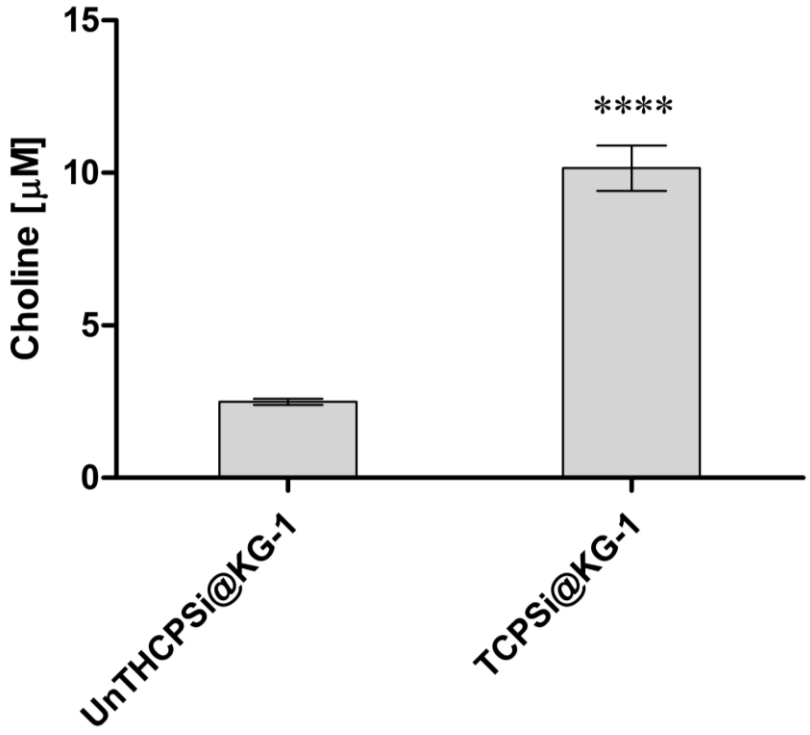

Figure 2. Lipid assay. Concentration of choline in 1 mg of particles after extrusion, quantified with the kit to measure the content of phosphatidyl choline. The results are presented as mean±s.d. (*n=3*). The sample was analyzed with one-way ANOVA followed by Bonferroni post-test and the level of significance was set at the probability of **** *p<0.0001*.

2.2. Stability Studies

An important parameter in the development of nanosystems is their stability both in physiological solutions (for safe and easy administration) and in biological fluids (plasma, synovial fluid). First, we evaluated the behavior of the NPs by DLS in two different physiological solutions: phosphate-buffered saline (PBS) 1X and glucose 5.4%, pH 7.4 (**Figure S4**). As for PBS, TCPSi@KG-1 and UnTHCPSi@KG-1 retain their size up to 30 min,

while their dimensions slightly increase after 1 h of incubation with the buffer. The positively charged APTS-TCPSi, however, also due to the partially exposed particles surface, show a high tendency to aggregate. In the case of isotonic glucose solution, hydrophobic UnTHCPSi@KG-1 are highly stable for the complete duration of the experiment, while with both TCPSi@KG-1 and APTS-TCPSi@KG-1, the presence of the sugar in the solution results in aggregation of the nanosystems.

The nanoplatform displaying a positive charge in the core of the biohybrid nanosystems showed the worst results in terms of stability, due to the only partial coating of the particles by the membranes. As previously reported for red blood cell membranes and positively charged polystyrene particles, the production of a nanosystem presenting a positively charged core encapsulated within a cell membrane is hampered by the presence of two opposite charges, the positive from the particles and the negative from the cell membranes.[12] Thereby, we focused the following experiments on the negatively charged particles, UnTHCPSi@KG-1 and TCPSi@KG-1.

The NPs intended to be administered intravenously should not aggregate in blood in order to prolong the circulation and take advantage of the extravasation through the ELVIS effect.[13] UnTHCPSi NPs not coated with the cytoplasmic membrane were not stable in fresh frozen plasma, aggregating to sizes > 1 μm immediately after being dispersed into it (**Figure 3a**). On the contrary, the presence of the cell membrane layer shields the particles, preventing the aggregation, and retaining an uniform size up to 2 h, with statistically significant differences compared to the uncoated particles. Interestingly, for TCPSi NPs (Figure 3b), the stabilizing effect of the cell membrane is weaker than the hydrophilicity of the surface, thus the coated and uncoated NPs displayed the same trend, with size values not statistically different. The size of both the systems, during the incubation with cytoplasmatic membranes increased to around 500 nm, with UnTHCPSi@KG-1 displaying lower standard deviation. The stabilizing effect of the cell membrane layer was more evident in UnTHCPSi NPs due to its more

hydrophobic surface, where the cell membrane stabilized the NPs, mimicking the cellular surface, while UnTHCPSi particles alone aggregate.[14]

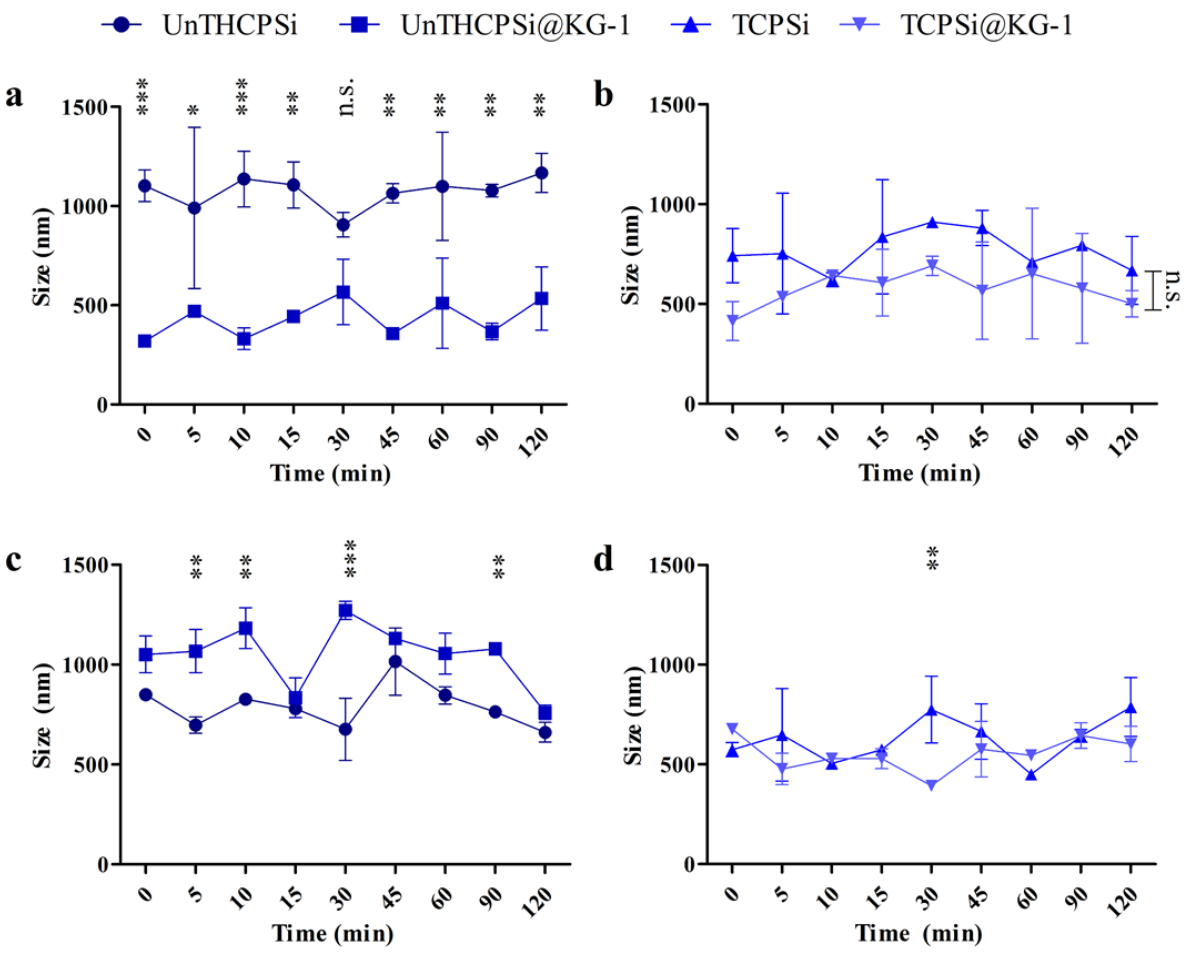

Figure 3. Stability of UnTCHPSi, UnTHCPSi@KG-1, TCPSi, and TCPSi@KG-1 systems in (a) and (b) human fresh frozen plasma, and (c) and (d) simulated synovial fluid, up to 2 h. The results are presented as mean±s.d. (*n=3*). The results were analyzed with two-way ANOVA, followed by Bonferroni's post-test and the levels of significance were set at the probabilities of *$p<0.05$, **$p<0.01$, and *** $p<0.001$.

Taking into account a possible intra-articular local administration, the stability of the biohybrid nanoplatforms in simulated synovial fluid was also evaluated.[15] However, as reported by a recent study, micro- and nano-particles administered locally, in the joint, will also distribute systemically.[16] The stabilizing effect due to the presence of the cell membrane

layer is limited for UnTHCPSi (Figure 3c), where the size of the coated particles increases to 800 nm, while the uncoated NPs form aggregates of 1 µm. Finally, when TCPSi both coated and uncoated are suspended in simulated synovial fluid (Figure 3d), they exhibited a similar trend between each other, *i.e.*, size increasing to 500–600 nm and remaining stable over 2 h.

2.3. Biological Assays

2.3.1. Cytocompatibility

Next, the cytocompatibility of the nanosystems was evaluated *in vitro*. We firstly evaluated the compatibility of the two nanosystems in the cells used to isolate the cell membranes, *i.e.*, KG-1 (**Figure 4a**). After 24 h, both coated and uncoated TCPSi were cytocompatible in the whole range of concentration assessed (0.5–500 µg mL^{-1}), while UnTHCPSi@KG-1 were cytocompatible only for the lower concentrations, with uncoated UnTHCPSi displaying a lower toxicity for higher concentrations. The cytocompatibility of the developed nanoplatforms was then assessed on cell lines representative of the target fibroblasts, present in the joint, endothelial cells (EA.hy926) representative of the cells lining the blood vessels, renal cells (HEK-293) and hepatic cells (HepG2) for the two main excretion routes.[17] All the NPs were cytocompatible when exposed to human dermal fibroblasts (Figure 4b), while the particles exhibited a surface-dependent cytotoxicity in EA.hy926 cells (Figure 4c). TCPSi NPs, both coated and uncoated, exhibited cytotoxicity, with the coated nanosystems inducing reduced viability at the highest concentrations (50 and 500 µg mL^{-1}). As for renal cells (Figure 4d), all the NPs induced a dose-dependent toxicity, particularly accentuated for both the coated and uncoated TCPSi NPs at the highest concentration assessed. Finally, in HepG2 cells, the hydrophilic TCPSi NPs displayed higher cytocompatibility at the lower concentrations, while all the NPs reduced the viability to 60% of the negative control at the highest concentration assessed (Figure 4e).

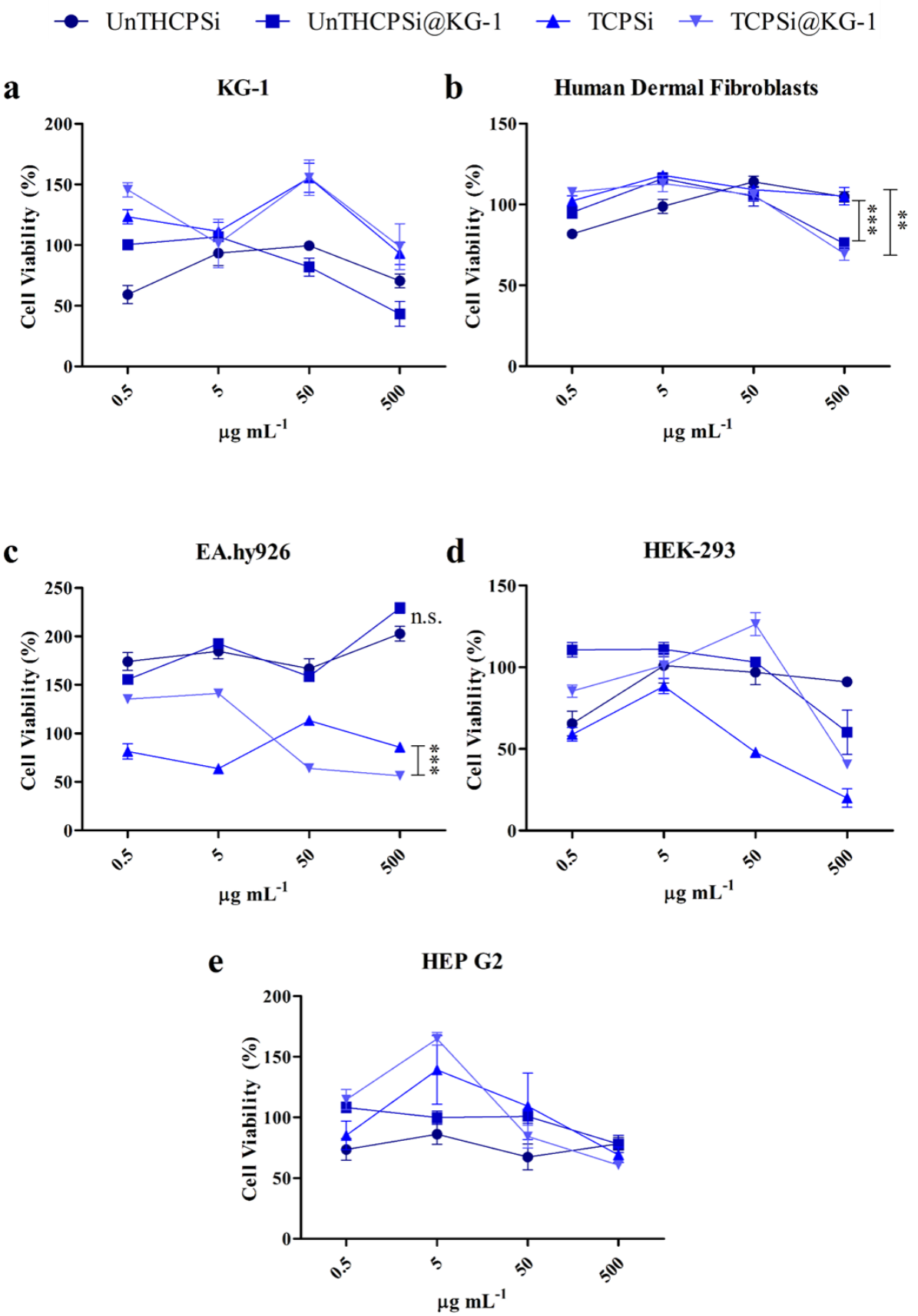

Figure 4. Cell viability (%) of (a) KG-1 cells, (b) human dermal fibroblast, (c) EA.hy926, (d) HEK-293, (e) HepG2 incubated with UnTHCPSi, UnTHCPSi@KG-1, TCPSi, and

TCPSi@KG-1 at different concentrations for 24 h. Complete medium and Triton X-100 (1%) were used as negative and positive control, respectively. The results are presented as mean±s.d. ($n \geq 3$). The samples were analyzed with two-way ANOVA, followed by Bonferroni's post-test and the levels of significance were set at the probabilities of ** $p < 0.01$ and *** $p < 0.001$.

After 48 h of incubation, all the nanosystems resulted in a pronounced dose-dependent cytotoxicity on KG-1 macrophages (**Figure 5a**), starting from 50 μg mL^{-1} for UnTHCPSi@KG-1 and involving all the NPs at the highest concentration. Even after prolonged incubation, fibroblasts did not exhibit significant decrease in the cell viability due to the NPs, with all the nanosystems being cytocompatible over the whole range of concentrations tested (Figure 5b). The same trend was observed also in the endothelial cells, EA.hy926, where the surface-dependent difference seen for shorter incubation times (Figure 4c) was not found for longer incubation times (Figure 5c). The effect of the incubation of the nanosystems for 48 h on HEK-293 displayed a dose-dependent cytotoxicity at the highest concentration assessed (500 μg mL^{-1}), while at the lower concentrations they were cytocompatible (Figure 5d). Finally, after 48 h of incubation with the nanosystems, HepG2 cells were more sensitive to the hydrophobic UnTHCPSi NPs both coated and uncoated, compared to the hydrophilic TCPSi ones (Figure 5e).

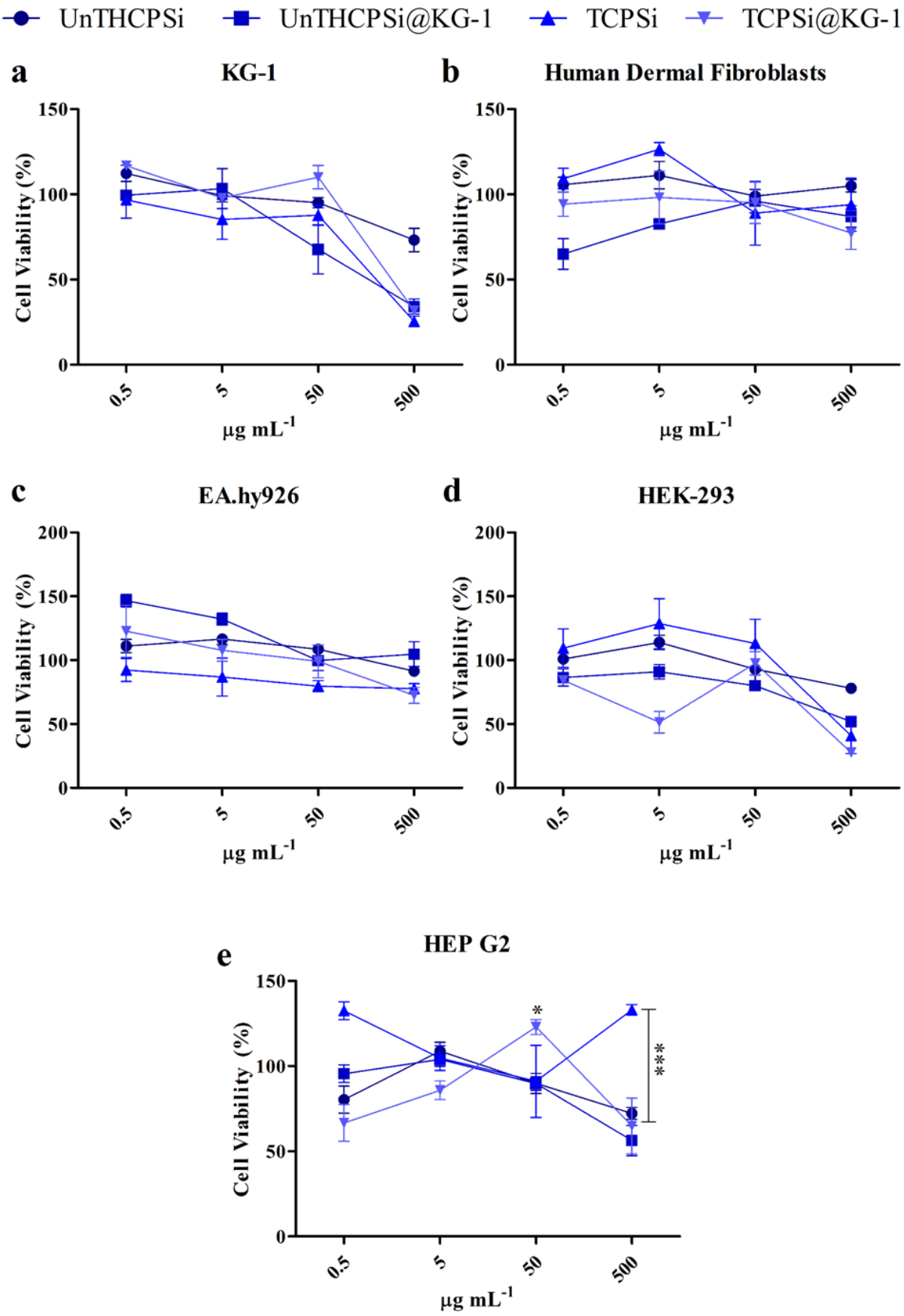
UnTHCPSi
UnTHCPSi@KG-1
TCPSi
TCPSi@KG-1
a
KG-1
b
Human Dermal Fibroblasts
c
EA.hy926
d
HEK-293
e
HEP G2
Cell Viability (%)
µg mL-1
0.5
5
50
500
0
50
100
150
200
*
***

Figure 5. Cell viability (%) of (a) KG-1 cells, (b) human dermal fibroblast, (c) EA.hy926, (d) HEK-293, and (e) HepG2 incubated with UnTHCPSi, UnTHCPSi@KG-1, TCPSi, and TCPSi@KG-1 at different concentrations for 48 h. Complete medium and Triton X-100 (1%) represented the negative and positive control, respectively. The results are presented as mean±s.d. ($n \geq 3$). The samples were analyzed with two-way ANOVA, followed by Bonferroni's post-test and the levels of significance were set at the probabilities of $*p<0.05$ and *** $p<0.001$.

2.3.2 Immunological Profile

The nanosystems employed for the treatment of autoimmune diseases should exhibit an immunoneutral profile, avoiding a further activation of the immune system.[18] Thus, we sought to investigate the immunological profile of the developed nanoplatforms, before and after coating with the cytoplasmatic membranes. As shown in **Figures 6a** and **c**, after 48 and 72 h of incubation, UnTHCPSi NPs induced a statistically significant ($p<0.001$) enhanced presentation of CD80 on KG-1 cells. However, the coating with cell membrane greatly reduced the immunostimulation to the levels of the control. It was previously shown that the hydrophobic surface of UnTHCPSi NPs is mildly stimulating antigen presenting cells (as measured by the presentation of co-stimulatory signals and the secretion of pro-inflammatory cytokines), while the hydrophilic surface of TCPSi NPs did not result in any activation input.[4e] As for CD86 (Figures 6b and d), all the nanosystems, except TCPSi, showed a significant difference compared to the control after 48 h, but not after longer incubation time (72 h).

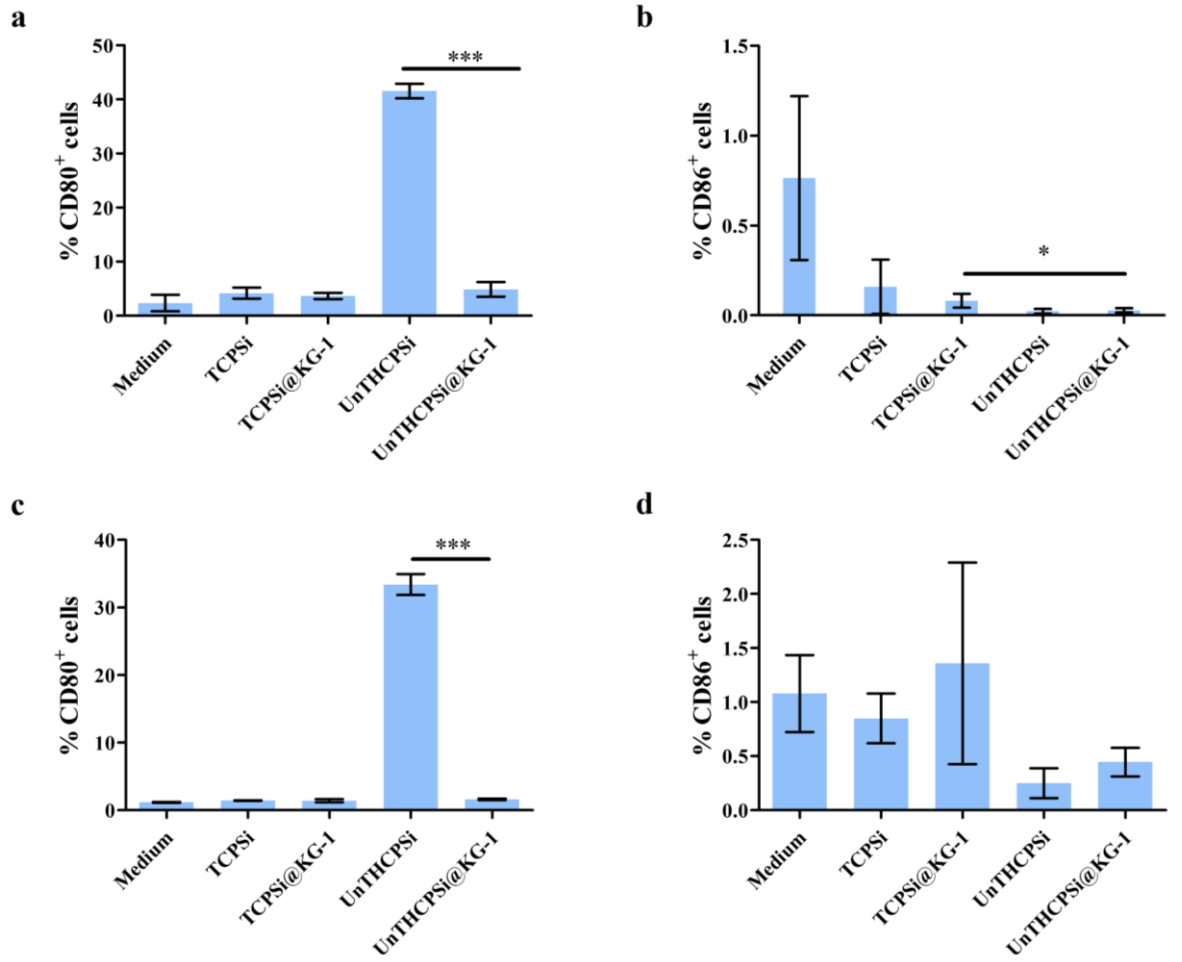

Figure 6. Percentage of cells presenting CD80 after 48 h (a) and 72 h (c) or CD86 after 48 h (b) and 72 h (d). The cells were incubated with the nanosystems at a concentration of 50 µg mL^{-1} for 48 h or 72 h, and then stained with PE-antihuman CD80 and APC-antihuman CD86 antibodies. The results are presented as mean±s.d (*n=3*). The data were analyzed by one-way ANOVA followed by Bonferroni's post-test and the levels of significance were set at the probabilities of *$p<0.05$* and ***$p<0.001$*. In (a) and (c) the samples of the UnTHCPSi NPs were compared to the sample UnTHCPSi@KG-1, while in (b) the samples were compared to the control (medium).

3. Conclusion

A study of the parameters influencing the production of PSi@cytoplasmic membranes was conducted. Positively charged PSi NPs showed a lower degree of encapsulation due to the strong electrostatic interactions between the particles and the cell membranes. As for the

differences in the hydrophobicity of the surface of the NPs, they had an impact on the choice of the medium employed in the extrusion and in the additional procedures (tip sonication) required. The nanoplatforms showed acceptable stability in physiological buffers, while in plasma and simulated synovial fluid greatly enhanced the stability of the hydrophobic particles (UnTHCPSi). Moreover, the cytocompatibility of the systems evaluated in different cell lines representing the cells present in the target organs, blood vessel and the kidney and liver. The nanoplatforms were compatible up to 48 h at concentrations ranging from 0.5 to 50 μg mL^{-1}. Finally, the immunological profile investigated in KG-1 macrophages showed that PSi@KG-1 nanosystem did not result in the activation of the immune system and the coating of UnTHCPSi particles with cell membranes attenuated the immunostimulative potential of the particles. Overall, we developed, as proof of concept, two biohybrid cytocompatible nanoplatforms as potential drug delivery systems or as antigen carriers for the induction of tolerance against autoimmune diseases.

4. Experimental Section

Preparation of PSi nanoparticles: Silicon NPs were prepared by electrochemical etching of Si wafers and their surface was subsequently modified to obtain thermal hydrocarbonization followed by modification with an alkenoic acid (undecylenic acid, UnTHCPSi) to provide terminal carboxylic acid groups, or thermal carbonization (TCPSi) and thermal carbonization followed by a hydroxyl generation step and silanization using (3-aminopropyl)-triethoxysilane (APTS-TCPSi) to introduce available amine groups, as previously reported.[4a, 4b, 4d, 4e, 14a, 19] Nitrogen sorption at −196°C (TriStar 3000, Micromeritic, USA) was used to obtain the specific surface area (SSA) using the BET method and the total pore volume (at a relative pressure of 0.97) of the NPs. The properties of the initial particles are shown in **Table 2**.

Table 2. Surface modification, average hydrodynamic diameter, indicative number of NPs per mg of material, SSA, pore volume, and average pore diameter for each of the PSi NPs employed in this work.

Particle	Surface modification	Size [nm]	Particles per mg	SSA [m^2g^{-1}]	Volume [cm^3g^{-1}]	Average Pore Diameter [nm]
TCPSi	Thermally Carbonized	159.8	9.96×10^{12}	212±4	0.52±0.07	9.9±1.4
UnTHCPSi	Undecylenic Thermally Hydrocarbonized	140.5	1.30×10^{13}	305±10	0.89±0.01	11.6±0.4
APTS-TCPSi	(3-aminopropyl)-triethoxysilane modified thermally carbonized	187.0	3.68×10^{12}	331±8	0.89±0.07	11.1±0.7

Cell lines: KG-1 macrophages (ATCC® CCL-246™) served as source of cell membrane, while we evaluated the cytocompatibility in human dermal fibroblasts, EA.hy926 (ATCC® CRL-2922™), HEK-293 (ATCC® CRL-1573™), and HepG2 (ATCC® HB-8065™). The cells were cultured according to the ATCC protocols.

Isolation of cell membrane: We proceeded to the isolation of the cells membrane from KG-1 macrophages as widely reported.[14, 15] Briefly, about 3×10^6 cells were washed three times with PBS 1X and resuspended in lysing buffer (Tris HCl, KCl, $MgCl_2$, all from Sigma Aldrich, USA), followed by ultracentrifugation to isolate the cell membranes.

Preparation of PSi@KG-1 particles: PSi NPs were encapsulated within cell membrane vesicles by membrane extrusion (polycarbonate membrane, pore size 0.8 μm, Nucleopore Track-Etch Membrane, Whatman, UK) through an extruder (Avanti Polar Lipids Inc., USA).

For the APTS-TCPSi@KG-1 NPs 1 mL of sucrose (0.3 M; Sigma Aldrich, USA) was employed to resuspend the cell membranes. 1 mg of PSi NPs were resuspended in this solution, tip sonicated (10 s, 30% amplitude; Ultrasonic Processor VCX series, Sonics and Material Inc., USA), and extruded for 21 passages. The solution collected from the extruded was tip sonicated a second time (10 s, 30% amplitude).

For the TCPSi@KG-1 NPs the cell membranes were suspended in 1 mL of Milli-Q water (Millipore, USA). Then, 0.5 mg of the TCPSi particles were added, and the solution was tip sonicated (10 s, 30% amplitude) prior to extrusion for 21 passages.

For the UnTHCPSi@KG-1 NPs the cell membranes were recovered in 1 mL of sucrose (0.3 M, Sigma Aldrich, USA), added in 1 mg of UnTHCPSi NPs, and tip sonicated the solution (10 s, 30 % amplitude) before passing the sample through the extruder for 21 times. The solution recovered from the extruder was tip sonicated again, keeping the parameters constant.

Lipid assay: In order to quantify the amount of lipid encapsulating the particles, we performed a lipid assay for the quantification of choline in the phosphocholine lipids in the membrane using a phosphatidylcholine assay kit (Sigma Aldrich, USA), according to the manufacturer's instructions. Briefly, after incubation of the complete system with the reagents, the suspensions were centrifuged at 16 100 *g*, to separate PSi nanoparticles from the cell membrane lipids reacted. This step was performed in order to avoid interferences, deriving from the particles, in the fluorescence reading.

Dynamic light scattering (DLS) and electrophoretic light scattering (ELS): The average hydrodynamic diameter, polydispersity index (PdI), zeta (ζ)-potential, and stability of the

formulations developed in different buffers were evaluated by DLS and ELS, using a Zetasizer Nano ZS (Malvern Instrument Ltd., UK). Briefly, 25 µL of particle solution (1 mg mL^{-1} for UnTHCPSi and APTS-TCPSi; 0.5 mg mL^{-1} for TCPSi) were diluted in 975 µL of Milli-Q water prior to each measurement.

Transmission electron microscope (TEM): The shape of the nanosystems were imaged with a TEM (Jeol 1400, Japan) microscope at 80.0 KeV. In brief, about 5 µL of a solution containing the samples were applied to a carbon-coated copper grid (Electron Microscope FCF 200-CU Mesh Copper) for 5 min, before removing the excess with filter paper and overnight drying. The pictures were analyzed with ImageJ software (NIH, USA) to determine the size of the particles (10 particles measured for each sample).

Scanning electron microscope (SEM) with energy dispersive X-rays (EDX) analysis: The elemental composition of the formulations was analyzed by EDX (Oxford INCA 350, Oxford Instruments, UK) connected with a SEM (Hitachi S-4800, Hitachi, Japan) at 30.0 KeV. The samples were applied to carbon-coated copper grids (as for the TEM imaging).

Stability of the system in different buffers: The stability of the system in different buffers was evaluated by measuring the changes in size and surface potential upon incubation over time. Firstly, we investigated the stability up to 1 h in physiological buffers suitable for administration of the systems: PBS 1X and glucose 5.4% (pH 7.4). About 200 µL of each sample were added to 1 mL of the buffer solution. The samples were incubated at room temperature, with aliquots taken at different time points, up to 1 h. In order to evaluate the stability of the system in biological conditions following an intravenous administration, we tested the stability of the systems in fresh frozen plasma (provided by Finnish Red Cross), up to 2 h. The FFP was thawed, centrifuged at 6000 rpm, and filtered through a 0.2 µm filter (0.2

μm sterile Acrodisc® Syringe Filters with Supor® Membrane, Pall Corporation, USA) before use. About 300 μL of each sample were pipetted in 1.5 mL of fresh frozen plasma, and stirred at 200 rpm and 37°C. Aliquots were taken at different times during the incubation period.

Finally, with the aim of a possible application in rheumatoid arthritis, the behavior of the nanosystems in simulated synovial fluid (SSF) was also evaluated. Simulated synovial fluid was prepared as previously described.[23] In particular, we used the buffer prepared with modified Hank's Balanced Salt Solution–N-[2-hydroxyethyl]piperazine-N'-[2-ethanesulfonic acid] (HBSS–HEPES, 0.14 M of NaCl; 5.4 mM of KCl; 1.62 mM of $CaCl_2$; 4.16 mM of $NaHCO_3$; 2.7 mM of $Na_2HPO_4.2H_2O$; 0.49 mM of $MgCl_2.6H_2O$; without glucose; pH 8.0; all the chemicals are from Sigma Aldrich, USA) and bovine serum albumin (4 mg mL^{-1}, Sigma Aldrich, USA), pH 8.0. The SFF was filtered with a 0.2 μm filter (0.2 μm sterile Acrodisc® Syringe Filters with Supor® Membrane, Pall Corporation, USA) before use. About 300 μL of each sample were pipetted in 1.5 mL of SSF and stirred at 200 rpm and 37°C. Aliquots were taken at different time points, up to 2 h.

Cytocompatibility assay: The cytocompatibility of the nanosystems was evaluated on the following cell lines: KG-1, human dermal fibroblasts, EA.hy926, HEK-293, and HepG2. Complete medium and Triton X-100 (1%) were used as negative and positive control, respectively. In brief, adherent cells were seeded at the density of about 2×10^5 cells per mL in 96-well plates (Corning, USA) and left attaching overnight. The samples were diluted in complete medium. The medium was removed from the well, the samples were added to the appropriate wells, and the plate was incubated at 37°C. For KG-1, about 50 μL of a 4×10^5 cells per mL were added to each well, followed by 50 μL of the samples at double concentration and the plate was then incubated at 37°C.

We assessed the effect of the formulation on the cellular viability by an ATP-luciferase assay (Cell Titer Glo®, Promega, USA). As for adherent cells, upon completion of the incubation,

the medium was removed and the wells were washed twice with HBSS–HEPES (pH 7.4), before adding 100 μL of a 1:1 CellTiter Glo®:HBSS–HEPES solution to each well. In the case of KG-1, 100 μL of CellTiter Glo® were added to each well directly. The luminescence was then read with a Varioskan Lux multimodal plate reader (Thermo Fisher, USA).

Immunological profile of the NPs: We evaluated the immunological profile of the formulations by measuring the changes in the expression of co-stimulatory markers, CD80 and 86, in KG-1 macrophages. KG-1 were seeded at a density of 4×10^5 cells per mL in 12-well plates (Corning, USA) and the samples, at double concentration, were added to the appropriate wells. Complete medium and LPS (100 ng mL^{-1}) were used as negative and positive control, respectively. The cells were then incubated for 48 or 72 h. We centrifuged the cells and stained them with anti-human CD80-PE and CD86-APC antibodies (BD Biosciences, USA), washed twice and analyzed them with LSR II flow cytometer (BD Biosciences, USA).

Statistical analysis: We report the results as mean ± s.d. ($n \geq 3$). The data were analyzed with two-way ANOVA followed by the Bonferroni post-test or one-way ANOVA followed by the Bonferroni post-test, as indicated in the Figures' caption, using Graphpad Prism 5 (GraphPad Software Inc, USA). The levels of significance were set at probabilities of $*p<0.05$, $**p<0.01$ and $***p<0.001$.

Supporting Information

Supporting Information is available from the Wiley Online Library or from the author.

Acknowledgements

H.A.S. acknowledges financial support from the University of Helsinki Research Funds, the Sigrid Jusélius Foundation (decision no. 4704580), the HiLIFE Research Funds, and the

European Research Council under the European Union's Seventh Framework Programme (FP/2007-2013, grant no. 310892).

Conflict of Interest

The authors declare no conflict of interest.

Received: ((will be filled in by the editorial staff))
Revised: ((will be filled in by the editorial staff))
Published online: ((will be filled in by the editorial staff))

References

[1] S. Banskota, P. Yousefpour, A. Chilkoti, *Macromol Biosci* **2017**, 17.
[2] a) C. M. Hu, L. Zhang, S. Aryal, C. Cheung, R. H. Fang, L. Zhang, *Proc Natl Acad Sci U S A* **2011**, 108, 10980; b) E. Chambers, S. Mitragotri, *J Control Release* **2004**, 100, 111; c) M. T. Stephan, S. B. Stephan, P. Bak, J. Chen, D. J. Irvine, *Biomaterials* **2012**, 33, 5776.
[3] a) R. H. Fang, C. M. Hu, B. T. Luk, W. Gao, J. A. Copp, Y. Tai, D. E. O'Connor, L. Zhang, *Nano Lett* **2014**, 14, 2181; b) W. Gao, C. M. Hu, R. H. Fang, B. T. Luk, J. Su, L. Zhang, *Adv Mater* **2013**, 25, 3549; c) C. M. Hu, R. H. Fang, K. C. Wang, B. T. Luk, S. Thamphiwatana, D. Dehaini, P. Nguyen, P. Angsantikul, C. H. Wen, A. V. Kroll, C. Carpenter, M. Ramesh, V. Qu, S. H. Patel, J. Zhu, W. Shi, F. M. Hofman, T. C. Chen, W. Gao, K. Zhang, S. Chien, L. Zhang, *Nature* **2015**, 526, 118; d) J.-G. Piao, L. Wang, F. Gao, Y.-Z. You, Y. Xiong, L. Yang, *ACS Nano* **2014**, 8, 10414.
[4] a) M. P. A. Ferreira, S. Ranjan, S. Kinnunen, A. Correia, V. Talman, E. Makila, B. Barrios-Lopez, M. Kemell, V. Balasubramanian, J. Salonen, J. Hirvonen, H. Ruskoaho, A. J. Airaksinen, H. A. Santos, *Small* **2017**, 13; b) N. Shrestha, F. Araújo, M. A. Shahbazi, E. Mäkilä, M. J. Gomes, B. Herranz‐Blanco, R. Lindgren, S. Granroth, E. Kukk, J. Salonen, *Adv Funct Mater* **2016**, 26, 3405; c) M.-A. Shahbazi, N. Shrestha, E. Mäkilä, F. Araújo, A. Correia, T. Ramos, B. Sarmento, J. Salonen, J. Hirvonen, H. A. Santos, *Nano Research* **2015**, 8, 1505; d) B. Herranz‐Blanco, D. Liu, E. Mäkilä, M. A. Shahbazi, E. Ginestar, H. Zhang, V. Aseyev, V. Balasubramanian, J. Salonen, J. Hirvonen, *Adv Funct Mater* **2015**, 25, 1488; e) M. A. Shahbazi, T. D. Fernandez, E. M. Makila, X. Le Guevel, C. Mayorga, M. H. Kaasalainen, J. J. Salonen, J. T. Hirvonen, H. A. Santos, *Biomaterials* **2014**, 35, 9224; f) A. Parodi, N. Quattrocchi, A. L. Van De Ven, C. Chiappini, M. Evangelopoulos, J. O. Martinez, B. S. Brown, S. Z. Khaled, I. K. Yazdi, M. V. Enzo, *Nature Nanotechnol* **2013**, 8, 61.
[5] a) V. Balasubramanian, A. Correia, H. Zhang, F. Fontana, E. Mäkilä, J. Salonen, J. Hirvonen, H. A. Santos, *Adv Mater* **2017**, 29; b) F. Fontana, M. A. Shahbazi, D. Liu, H. Zhang, E. Makila, J. Salonen, J. T. Hirvonen, H. A. Santos, *Adv Mater* **2017**, 29.
[6] a) L. Northrup, M. A. Christopher, B. P. Sullivan, C. Berkland, *Adv Drug Deliv Rev* **2016**, 98, 86; b) P. Serra, P. Santamaria, *Clin Immunol* **2015**, 160, 3.
[7] I. B. McInnes, G. Schett, *Lancet* **2017**, 389, 2328.

[8] a) S. Dolati, S. Sadreddini, D. Rostamzadeh, M. Ahmadi, F. Jadidi-Niaragh, M. Yousefi, *Biomed Pharmacother* **2016**, 80, 30; b) E. Nogueira, A. C. Gomes, A. Preto, A. Cavaco-Paulo, *Nanomedicine* **2016**, 12, 1113.

[9] X. Clemente-Casares, J. Blanco, P. Ambalavanan, J. Yamanouchi, S. Singha, C. Fandos, S. Tsai, J. Wang, N. Garabatos, C. Izquierdo, S. Agrawal, M. B. Keough, V. W. Yong, E. James, A. Moore, Y. Yang, T. Stratmann, P. Serra, P. Santamaria, *Nature* **2016**, 530, 434.

[10] I. A. Udalova, A. Mantovani, M. Feldmann, *Nat Rev Rheumatol* **2016**, 12, 472.

[11] S. G. Wolf, P. Rez, M. Elbaum, *J Microsc* **2015**, 260, 227.

[12] B. T. Luk, C.-M. J. Hu, R. H. Fang, D. Dehaini, C. Carpenter, W. Gao, L. Zhang, *Nanoscale* **2014**, 6, 2730.

[13] a) A. Sen Gupta, *Wiley Interdiscip Rev Nanomed Nanobiotechnol* **2016**, 8, 255; b) C. Li, H. Li, Q. Wang, M. Zhou, M. Li, T. Gong, Z. Zhang, X. Sun, *J Control Release* **2017**, 246, 133.

[14] a) M. A. Shahbazi, P. V. Almeida, E. M. Makila, M. H. Kaasalainen, J. J. Salonen, J. T. Hirvonen, H. A. Santos, *Biomaterials* **2014**, 35, 7488; b) J. S. Gebauer, M. Malissek, S. Simon, S. K. Knauer, M. Maskos, R. H. Stauber, W. Peukert, L. Treuel, *Langmuir* **2012**, 28, 9673.

[15] N. Diomidis, S. Mischler, N. More, M. Roy, S. Paul, *Wear* **2011**, 271, 1093.

[16] J. Pradal, P. Maudens, C. Gabay, C. A. Seemayer, O. Jordan, E. Allemann, *Int J Pharm* **2016**, 498, 119.

[17] a) C. He, Y. Hu, L. Yin, C. Tang, C. Yin, *Biomaterials* **2010**, 31, 3657; b) L. Huo, R. Chen, L. Zhao, X. Shi, R. Bai, D. Long, F. Chen, Y. Zhao, Y. Z. Chang, C. Chen, *Biomaterials* **2015**, 61, 307; c) M. C. Kraan, J. J. Haringman, H. Weedon, E. C. Barg, M. D. Smith, M. J. Ahern, T. J. Smeets, F. C. Breedveld, P. P. Tak, *Ann Rheum Dis* **2004**, 63, 483; d) A. Mor, S. B. Abramson, M. H. Pillinger, *Clin Immunol* **2005**, 115, 118.

[18] M. Gharagozloo, S. Majewski, M. Foldvari, *Nanomedicine* **2015**, 11, 1003.

[19] L. M. Bimbo, M. Sarparanta, H. A. Santos, A. J. Airaksinen, E. Makila, T. Laaksonen, L. Peltonen, V. P. Lehto, J. Hirvonen, J. Salonen, *ACS Nano* **2010**, 4, 3023.

Biomimetic nanoplatforms composed of porous silicon particles and vesicles derived from the cytoplasmatic membrane of macrophages are developed. The platforms are characterized in terms of size, surface charge, and uniformity of coating. The stability of the systems in physiological fluids is investigated, highlighting an improvement after coating with the cell membrane. The nanoplatforms showed cytocompatibility and an immunological neutral profile.

Bioengineered platforms

Flavia Fontana*, Silvia Albertini, Alexandra Correia, Marianna Kemell, Rici Lindgren, Ermei Mäkilä, Jarno Salonen, Jouni T. Hirvonen, Franca Ferrari and Hélder A. Santos*

Bioengineered Porous Silicon Nanoparticles@Macrophages Cell Membrane as Composite Platforms for Rheumatoid Arthritis

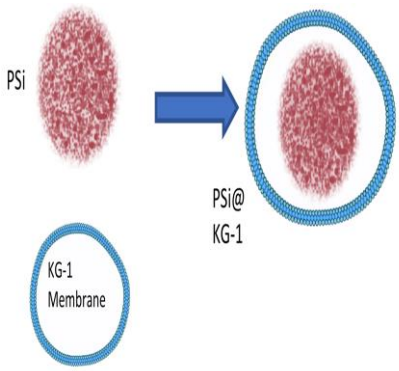

Scheme 1

Fig. 1

Fig. 2

Fig. 3


Click here to access/download
Production Data
Figura 3 final.tif

Fig. 4

Fig. 5


Click here to access/download
Production Data
Figure 5 final.tif

Graphical Abstract